A Fully Defined Yeast iVT tRNA Translation Platform and the Synergistic Role of eIF5A and Mg2+

Author: Yuanhan Jin

Affiliation: School of Medicine, Southeast of University

Abstract

We reconstructed Saccharomyces cerevisiae translation with a fully synthetic panel of twenty-one in-vitro-transcribed tRNAs, one isoacceptor per canonical amino acid plus the initiator species. This minimal pool decodes all sixty-one sense codons and, after individual aminoacylation, drives peptide synthesis in a defined yeast PURE system at yields comparable to native tRNAs. Long peptides stall unless supplemented; adding either eukaryotic factor eIF5A or elevated Mg2+ restores activity, and their combination increases Nano luciferase output about fivefold. Alanine scanning shows that basic residues R27 and R87 within the eIF5A core, rather than the hypusine side chain, provide the principal P-site tRNA stabilization. Higher magnesium alone accelerates elongation but raises UAG and UGA read-through to roughly fifteen percent, revealing a trade-off between speed and fidelity when tRNAs are unmodified. Installing t6A37 or m1G37 on selected synthetic tRNAs further improves processivity. The resulting minimal yet programmable yeast platform enables systematic dissection of modification roles and rapid genetic-code engineering.

Keywords：IVT tRNA; eIF5A; Mg2+; Yeast; Translation

Introduction

Translation accuracy relies on the coordinated function of tRNAs, ribosomes, and elongation factors. Traditional cell lysates obscure detailed functional analyses due to their inherent complexity. PURE (Protein synthesis Using Recombinant Elements) systems overcome these limitations by using recombinantly produced and purified components, enabling precise control of the translation process [1]. Previous bacterial PURE systems showed that minimal sets of 21 tRNAs could theoretically decode all codons through wobble pairing [2]. However, extending this minimal set to eukaryotic systems faces challenges due to stricter wobble rules and dependency on specific nucleotide modifications [3].

Eukaryotic translation elongation factor eIF5A and Mg2+ are key yet understudied factors influencing translation fidelity and processivity [4]. eIF5A, notably modified by hypusination, stabilizes P-site tRNAs during elongation. Meanwhile, Mg2+ modulates ribosome structure and decoding accuracy, affecting both elongation speed and fidelity [5].

This study aimed to establish a minimal, fully defined yeast PURE system using 21 in vitro transcribed yeast tRNAs, investigate the roles of eIF5A and Mg2+ in translation, and test the effects of specific tRNA modifications on translation efficiency and fidelity.

Materials and Methods

2.1 Plasmid Construction

Each yeast tRNA gene was individually cloned into the pCR4-TOPO vector between EcoRI restriction sites via PCR amplification, ligation, and transformation into XL10-Gold Ultracompetent Cells. Mutations of eIF5A were generated similarly using PCR quick-change methods based on pET-29b plasmids and validated by sequencing.

2.2 Preparation of iVT tRNAs

PCR amplification of yeast tRNA genes utilized primers including a T7 promoter. Transcription was performed using T7 RNA polymerase. Transcripts requiring processing (tRNAMetiCAU, tRNAAspGUC, tRNAGluCUC, tRNATyrGUA) underwent trimming by E. coli RNase P. All synthesized iVT tRNAs were purified via HiTrap Q HP chromatography and confirmed by gel electrophoresis.

2.3 Preparation of Yeast S100 Fraction

Yeast strain YPH499 cells were cultured in YPD medium and lysed by mechanical grinding. The lysate was fractionated by ultracentrifugation at 20,000 × g, and subsequently at 100,000 × g, yielding the S100 fraction. This fraction underwent further purification through dialysis and Q-sepharose chromatography to remove nucleic acids, and the purified fractions were stored at -80°C.

2.4 Aminoacylation of iVT tRNAs

Purified iVT tRNAs were aminoacylated individually using optimized reaction conditions with yeast S100 fraction or recombinant aminoacyl-tRNA synthetases (e.g., E. coli MetRS, LysRS, GlnRS, yeast ProRS). Aminoacylation efficiency was quantified using radioactive-labeled amino acids followed by liquid scintillation counting.

2.5 Preparation and Purification of mRNA

DNA templates encoding desired peptides were amplified using PCR and transcribed in vitro by T7 RNA polymerase. mRNA transcripts were purified via phenol-chloroform extraction, ethanol precipitation, and desalination through MicroSpin columns.

2.6 Yeast PURE Translation System Reconstitution

The yeast translation system comprised purified recombinant ribosomes, elongation factors (eEF1A, eEF2, eEF3), release factors (eRF1, eRF3), aminoacylated iVT tRNAs, and synthesized mRNAs. Translation reactions were performed at 30°C for 3 hours, followed by analysis.

2.7 Peptide and Polypeptide Analysis

Translation products were analyzed by Tricine–SDS-PAGE. Visualization was facilitated using radioactive [35S]-methionine labeling and autoradiography. Enzymatic activities were assessed using Nano-Glo Luciferase assays, performed on GloMax detection systems.

2.8 Expression and Purification of eIF5A and Its Mutants

The eIF5A and mutant proteins were expressed in Rosetta (DE3) E. coli cells induced by IPTG. Proteins were purified via HiTrap Q HP chromatography, dialyzed into storage buffer, concentrated, aliquoted, and stored at -80°C.

2.9 Ribosome Binding Assays of eIF5A Mutants

The binding affinities of purified eIF5A proteins to yeast ribosomes were assessed through ultracentrifugation with sucrose cushion methods. Pelleted ribosomes were analyzed by SDS-PAGE followed by Western blotting using specific antibodies against eIF5A and ribosomal marker Asc1.

2.10 Site-specific tRNA Modifications (t6A37 and m1G37)

Specific nucleotide modifications (t6A37, m1G37) were introduced enzymatically using recombinant E. coli TsaB/C/D/E and TrmD enzymes. Modification efficiencies were verified using radiolabeled amino acids and MTase-Glo methyltransferase assays.

Results

Results

3.1 Design and Preparation of iVT tRNAs

A set of twenty-one minimal yeast anticodons were selected to decode all canonical amino acids, focusing on optimal decoding efficiency. Selected anticodons primarily began with G or C, except for Ala(UGC), Pro(UGG), and Ile(UAU) chosen for efficient aminoacylation. Unassigned codons were reserved for future genetic code expansion (Figure 1A). Synthesized tRNAs were produced by T7 transcription, processed when necessary, and purified. Aminoacylation efficiency of iVT tRNAs was confirmed to be comparable to native tRNAs (Figure 1B, C).

3.2 Functional Validation in Yeast PURE System

The prepared iVT tRNAs effectively supported short peptide translation, achieving comparable yields to native tRNAs. However, translation of longer polypeptides, such as nanoluciferase (225 amino acids), required supplementation with eIF5A or elevated Mg^{2+} for efficient translation (Figure 2A, B).

3.3 eIF5A and Mg^{2+} in Long Peptide Translation

eIF5A supplementation significantly enhanced the translation efficiency of long peptides, independently of its hypusination state. Both hypusine-modified and lysine-unmodified eIF5A variants promoted full-length translation efficiently (Figure 3A-D). Additionally, increasing Mg^{2+} concentration also facilitated elongation and full-length protein production even without eIF5A, although higher Mg^{2+} led to increased translation errors, including readthrough of stop codons (Figure 4A-D).

3.4 Translation Stalling and Intermediate Analysis

Analysis of translation products revealed frequent stalling during the synthesis of long peptides in low Mg^{2+} conditions and absence of eIF5A. SDS-PAGE and autoradiography suggested multiple stalling sites or incomplete elongation intermediates, demonstrating eIF5A's crucial role in stabilizing elongation complexes (Figure 5A-E).

3.5 Structural Insights of eIF5A Function

Residues R27 and R87 in eIF5A, rather than hypusine modification, proved essential for stabilizing the P-site tRNA during elongation. The double mutant R27E/R87E significantly reduced translation efficiency. Ribosome binding assays confirmed comparable binding affinity between wild-type and mutant eIF5A proteins, highlighting structural rather than binding differences (Figure 6A-C).

3.6 Mg^{2+} Effects on Translation Fidelity

Elevated Mg^{2+} concentrations markedly increased stop-codon readthrough during translation. Comparative analysis showed native and iVT tRNAs exhibited differences in codon preference and decoding accuracy. Optimal translation fidelity required moderate Mg^{2+} concentrations coupled with eIF5A supplementation (Figure 8A-G).

Discussion

The successful reconstitution of yeast translation with a minimal set of in vitro transcribed tRNAs represents a significant step toward a fully defined eukaryotic cell-free system. The selection of 21 minimal yeast anticodons demonstrated robust decoding capacity, confirming that minimal tRNA sets can effectively support translation, given careful anticodon selection to balance decoding efficiency and aminoacylation fidelity.

Our findings underscore the critical roles of eIF5A and Mg^{2+} in translation elongation. eIF5A significantly enhanced the translation of longer peptides, indicating its crucial role in stabilizing the elongation complex. Intriguingly, both hypusinated and unmodified eIF5A variants exhibited similar translation-promoting activities, suggesting the importance of structural features over the hypusine modification in facilitating elongation. Structural analyses further highlighted residues R27 and R87 as pivotal for the functional role of eIF5A in stabilizing the P-site tRNA, independent of hypusination.

The observed effects of Mg^{2+} highlight its dual role in translation efficiency and fidelity. Elevated Mg^{2+} concentrations increased elongation efficiency but also compromised translation fidelity by promoting stop-codon readthrough. This finding emphasizes the delicate balance necessary for optimal translation conditions and the importance of carefully tuning Mg^{2+} concentrations.

Furthermore, our study provides insights into translation stalling mechanisms, identifying frequent elongation pauses under low Mg^{2+} and eIF5A-deficient conditions. These stalling events underscore the necessity of factors stabilizing the elongation complex, revealing critical regulatory checkpoints within the translation process.

Lastly, the successful enzymatic installation of specific nucleotide modifications (t6A37 and m1G37) in iVT tRNAs significantly enhanced decoding fidelity and processivity. These modifications highlight the modular nature of our translation system, allowing targeted improvements in tRNA function. This flexibility opens avenues for future genetic code expansions and precise synthetic biology applications.

Overall, this work provides a foundational platform for systematically studying eukaryotic translation, enabling detailed analyses of translation mechanisms, elongation factor functions, and genetic code engineering.

References

1. Carlson ED, Gan R, Hodgman CE, Jewett MC. Cell-free protein synthesis: applications come of age. *Biotechnol Adv* 2012;30:1185-1194. DOI:10.1016/j.biotechadv.2011.09.016.
2. Shimizu Y et al. Cell-free translation reconstituted with purified components. *Nat Biotechnol* 2001;19:751-755. DOI:10.1038/90802.
3. Hodgman CE, Jewett MC. Optimized extract preparation methods and reaction conditions for improved yeast cell-free protein synthesis. *Biotechnol Bioeng* 2013;110:2643-2654.
4. Abe T et al. In vitro yeast reconstituted translation system reveals function of eIF5A for synthesis of long polypeptide. *J Biochem* 2020;167:451-462.
5. Korencić D, Söll D, Ambrogelly A. A one-step method for in vitro production of tRNA transcripts. *Nucleic Acids Res* 2002;30:e105.
6. de la Torre D, Chin JW. Reprogramming the genetic code. *Nat Rev Genet* 2021;22:169-

184.
7. Gutierrez E et al. eIF5A promotes translation of polyproline motifs. *Mol Cell* 2013;51:35-45.
8. Schuller AP et al. eIF5A functions globally in translation elongation and termination. *Mol Cell* 2017;66:194-205.
9. Schauss J et al. Magnesium contact ions stabilize the tertiary structure of tRNA. *J Phys Chem B* 2021;125:740-747.

Figure Legend

Figure 1. The codon-anti codon selection and constitution of iVT tRNAs.

(A) Left : The genetic codes of native yeast tRNAs; Right: selected anticodons for iVT tRNAs and the codons for the mRNA.

(B) The Urea-PAGE electrophoresis results of all kinds of puried iVT tRNAs, as well as the native tRNA mix (0.01 A_{260} units/lane). (C) Amino acid acceptance of each kinds of iVT tRNAs under optimal conditions, compared to the respective native tRNA.

Figure 2. The attempt of translation with iVT tRNAs, compared to the native yeast tRNA mix under 5 mM Mg^{2+} (without eIF5A). The concentration of native aa-tRNA in the yeast PURE system was 7.2 μM.

(A) The synthesis of HiBiT of nanoluciferse.

(B) The synthesis of full-length nanoluciferase.

Figure 3. Translation with iVT tRNAs in the presence of eIF5A under 5 mM Mg^{2+}. The activity of nanoluciferase was detected after 3hr reaction.

(A) The synthesis of HiBiT with iVT aa -tRNAs (14.4 μM) and

(B) native aa-tRNA (7.2 μM) in the presence of different concentrations of hypusinated eIF5A [eIF5A (hyp)] or unhypusinated eIF5A [eIF5A (lys)].

(C) The synthesis of full-length nanoluciferase with iVT aa -tRNAs and

(D) native aa-tRNA in the presence of different concentrations of eIF5A (hyp) or eIF5A (lys).

Figure 4. The effect of different concentrations of Mg^{2+} on the synthesis of full-length nanoluciferase in the absence or presence of 2.5 μM eIF5A (hyp) and eIF5A (lys). The nanoluciferase activity was detected after 3 hr reaction.

(A) The synthesis of nanoluciferase with iVT aa-tRNAs (14.4 μM) and

(B) native aa-tRNAs (7.2 μM) in the context of 5 mM, 7 mM and 9 mM Mg^{2+}. n=3.

(C) The Tricine SDS-PAGE electrophoresis of full-length product after 3hr reaction, with [35S] iVT aa-tRNAs and

(D) [^{35}S] native aa-tRNAs at the 5 mM Mg^{2+} and 9 mM Mg^{2+}.

Figure 5. The Tricine SDS-PAGE electrophoresis of nanoluciferase synthesis, using iVT aa-tRNAs (14.4 μM) in the absence or presence of 2.5 μM eIF5A (hyp). After 3hr reaction, the systems were treated with RNase A or not.

(A) The electrophoresis without mRNA.

(B) The electrophoresis of full-length nanoluciferase in the context of nanoluciferase mRNA at 5 mM Mg^{2+}.
(C) The electrophoresis of full-length nanoluciferase in the context of nanoluciferase mRNA without Flag sequence at 5 mM Mg^{2+}.
(D) The electrophoresis of full-length nanoluciferase in the context of nanoluciferase mRNA at 9 mM Mg^{2+}.
(E) The nanoluciferase activities of respective lanes in (A-D), detected after 3hr reaction.

Figure 6. The effect of eIF5A (lys) mutants on the synthesis of full-length nanoluciferase with iVT aa-tRNAs at 6 mM Mg^{2+}.
(A)The schematic structure of eIF5A interacting with P-site tRNA (from PBK: 5gak). The blue part is the body of eIF5A. The pink part is P-site tRNA. The violet part is hypusinated lysine of eIF5A. The red part is the 27th amino acid (lysine) on the body of eIF5A and the yellow part is the 87th amino acid (lysine).
(B) The synthesis ratio of nanoluciferase with iVT aa-tRNAs (14.4 μM) in the presence of different types of eIF5A (2.5 μM), in comparison with wild eIF5A (lys) (100%). n=3.
(C) The Western Blot of eIF5A and mutants binding with the yeast ribosome. The Asc1 was considered as the ribosome control. The concentration folds of eIF5A were compared to the constant concentration of ribosome (0.5 μM) in the reaction system.

Figure 7. The effect of eIF5A (lys) dual-site mutant on the translation of full-length nanoluciferase mRNA and [ProX4] inserted mRNA with native aa-tRNAs (7.2 μM) at 5mM Mg^{2+}. The mRNA sequences were designed according to our previous article.
(A)The translation of nanoluciferase mRNA and
(B) [ProX4] inserted mRNA with native aa-tRNAs, in the presence of 2.5 μM eIF5A (hyp), eIF5A (lys) and eIF5A (lys) R27E/R87E mutant.

Figure 8. Increasing Mg^{2+} levels in the yeast PURE system can improve the readthrough efficiency. The rates were calculated by the ratio of stop codons inserted mRNA with the normal full-length nanoluciferase mRNA (no motif), in the absence or presence of eRF1(0.5 μM). The nanoluciferase activities were collected after 1.5hr reaction. n=3.
(A)The readthrough rates with native aa-tRNAs (7.2 μM) in the absence of eIF5A (hyp) at the 5 mM Mg^{2+}.
(B) The readthrough rates with native aa-tRNAs in the presence of 2.5 μM eIF5A (hyp) at the 5 mM Mg^{2+}.
(C) The readthrough rates with native aa-tRNAs in the absence of eIF5A (hyp) at the 9 mM Mg^{2+}.
(D) The readthrough rates with native aa-tRNAs in the presence of 2.5 μM eIF5A (hyp) at the 9 mM Mg^{2+}.
(E) The readthrough rates with iVT aa-tRNAs (14.4 μM) in the presence of 2.5 μM eIF5A (hyp) at the 5 mM Mg^{2+}.
(F) The readthrough rates with iVT aa-tRNAs (14.4 μM) in the absence of eIF5A (hyp) at the 9 mM Mg^{2+}.
(G) The readthrough rates with iVT aa-tRNAs (14.4 μM) in the presence of 2.5 μM eIF5A (hyp)

at the 9 mM Mg^{2+}.

Supplementary Figure 1. The time course of the synthesis reaction under 5 mM Mg2+ in the presence of different concentrations of eIF5A (hyp) and eIF5A (lys), detected at the 1st hr, 2nd hr and 3rd hr.
(A)and (B) The synthesis of HiBiT with iVT aa-tRNA (14.4 μM) and native aa-tRNA (7.2 μM).
(C) and (D) The synthesis of full-length nanoluciferase with iVT aa-tRNA and native aa-tRNA.

Supplementary Figure 2. The time course of the synthesis of full-length nanoluciferase at different concentrations of Mg^{2+} in the absence or presence of 2.5 μM eIF5A (hyp) and eIF5A (lys).
(A)The synthesis of nanoluciferase at 5 mM, 7 mM and 9 mM Mg^{2+} with iVT aa-tRNAs, in the absence of eIF5A or the presence of (B) 2.5 μM eIF5A (hyp) and (C) eIF5A (lys).
(D) The synthesis of nanoluciferase at 5 mM, 7 mM and 9 mM Mg^{2+} with native aa-tRNAs, in the absence of eIF5A or the presence of (E) 2.5 μM eIF5A (hyp) and (F) eIF5A (lys).

Supplementary Figure 3. The time course of synthesis of full-length nanoluciferase with iVT aa-tRNAs (14.4 μM) in the absence or precence of different types of eIF5A (2.5 μM) at 6 mM Mg^{2+}.

Supplementary Figure 4. The time courses of readthrough assays in Figure 8. The nanoluciferase activities were collected after 1.5hr and 3hr reaction.
(A)The nanoluciferase activities in the context of native aa-tRNAs (7.2 μM) in the absence of eIF5A (hyp) at the 5 mM Mg^{2+}, with eRF1 or (B) without eRF1.
(C) The nanoluciferase activities in the context of native aa-tRNAs (7.2 μM) in presence of 2.5 μM eIF5A (hyp) at the 5 mM Mg^{2+}, with eRF1 or (D) without eRF1.
(E) The nanoluciferase activities in the context of native aa-tRNAs (7.2 μM) in the absence of 2.5 μM eIF5A (hyp) at the 9 mM Mg^{2+}, with eRF1 or (F) without eRF1.
(G) The nanoluciferase activities in the context of native aa-tRNAs (7.2 μM) in presence of 2.5 μM eIF5A (hyp) at the 9 mM Mg^{2+}, with eRF1 or (H) without eRF1.

Supplementary 5. The correlation analysis of nanoluciferase activities with input mRNA amount and reaction time. The synthesis of full-length nanoluciferase was performed with different concentrations of input mRNA (0.2 μM, 0.5 μM and 1 μM), in the presence of eRF1. The nanoluciferase activities were detected after 1.5 hr and 3 hr reaction.
(A)The synthesis of nanoluciferase with native aa-tRNAs (7.2 μM), in the absence and
(B) in the presence of 2.5 μM eIF5A (hyp) at 5 mM Mg^{2+}.
(C) The synthesis of nanoluciferase with native aa-tRNAs (7.2 μM), in the absence and

Figure 1

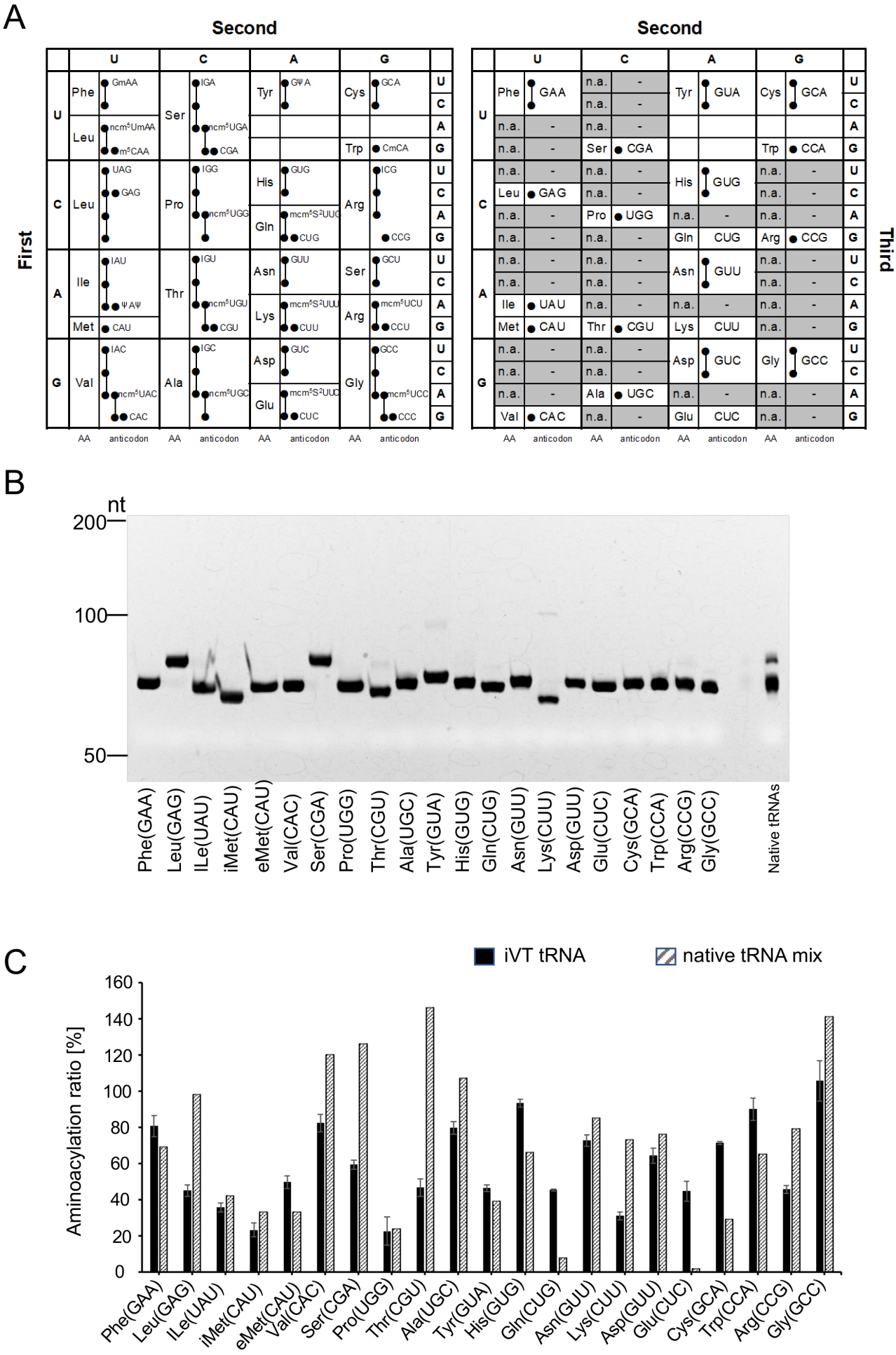
A
Second
First
Third
U
C
A
G
Phe
Leu
Ile
Met
Val
Ser
Pro
Thr
Ala
Tyr
His
Gln
Asn
Lys
Asp
Glu
Cys
Trp
Arg
Gly
GmAA
ncm5UmAA
m5CAA
UAG
GAG
IAU
ΨAΨ
CAU
IAC
ncm5UAC
CAC
IGA
ncm5UGA
CGA
IGG
ncm5UGG
IGU
ncm5UGU
CGU
IGC
ncm5UGC
GΨA
GUG
mcm5S2UUG
CUG
GUU
mcm5S2UUU
CUU
GUC
mcm5S2UUC
CUC
GCA
CmCA
ICG
CCG
GCU
mcm5UCU
CCU
GCC
mcm5UCC
CCC
GAA
GUA
GCA
CGA
CCA
GAG
UGG
CUG
CCG
UAU
CAU
CGU
CUU
GUC
GCC
UGC
CUC
n.a.
-
AA
anticodon
B
nt
200
100
50
Phe(GAA)
Leu(GAG)
ILe(UAU)
iMet(CAU)
eMet(CAU)
Val(CAC)
Ser(CGA)
Pro(UGG)
Thr(CGU)
Ala(UGC)
Tyr(GUA)
His(GUG)
Gln(CUG)
Asn(GUU)
Lys(CUU)
Asp(GUU)
Glu(CUC)
Cys(GCA)
Trp(CCA)
Arg(CCG)
Gly(GCC)
Native tRNAs
C
iVT tRNA
native tRNA mix
Aminoacylation ratio [%]
160
140
120
100
80
60
40
20
0
Phe(GAA)
Leu(GAG)
ILe(UAU)
iMet(CAU)
eMet(CAU)
Val(CAC)
Ser(CGA)
Pro(UGG)
Thr(CGU)
Ala(UGC)
Tyr(GUA)
His(GUG)
Gln(CUG)
Asn(GUU)
Lys(CUU)
Asp(GUU)
Glu(CUC)
Cys(GCA)
Trp(CCA)
Arg(CCG)
Gly(GCC)

Figure 2

A

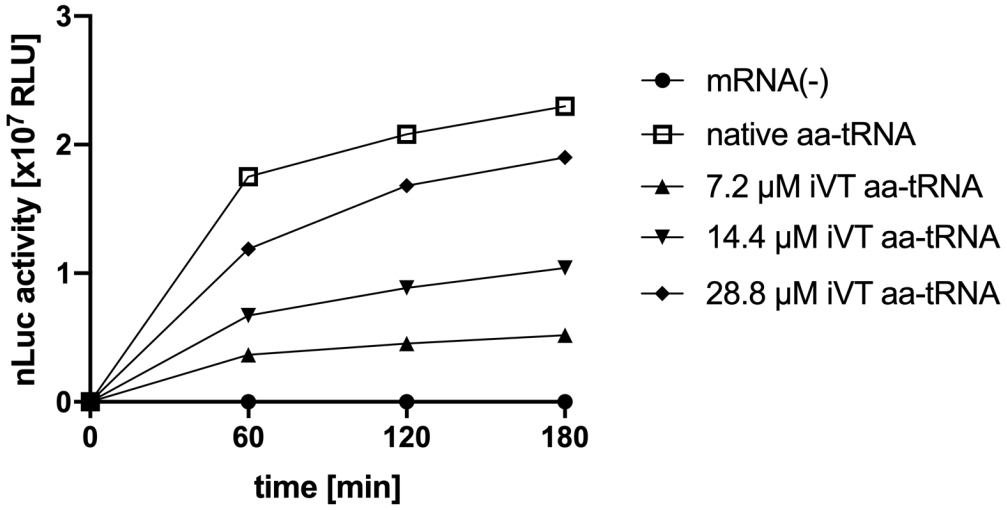
nLuc activity [x10^7 RLU]
3
2
1
0
0
60
120
180
time [min]
mRNA(-)
native aa-tRNA
7.2 μM iVT aa-tRNA
14.4 μM iVT aa-tRNA
28.8 μM iVT aa-tRNA

B

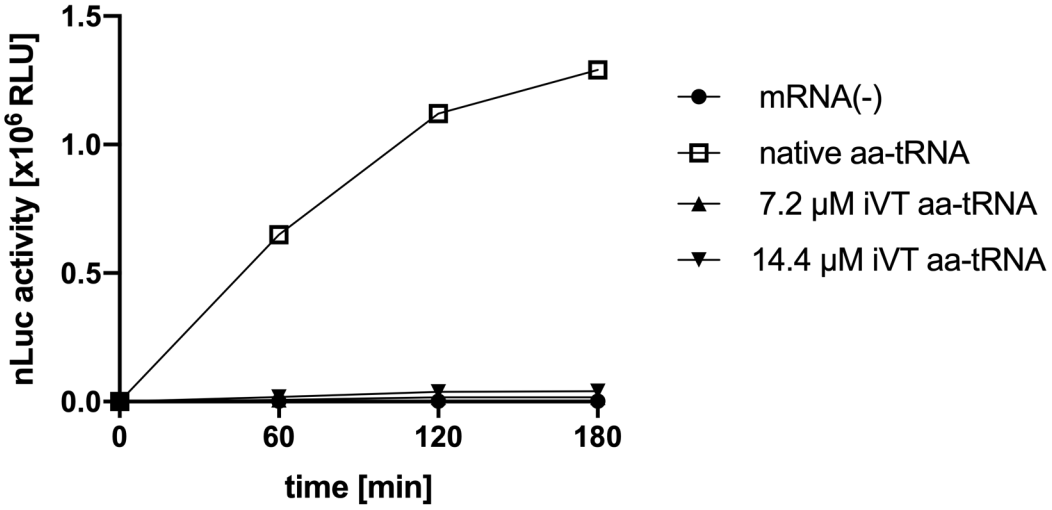
nLuc activity [x10^6 RLU]
1.5
1.0
0.5
0.0
0
60
120
180
time [min]
mRNA(-)
native aa-tRNA
7.2 μM iVT aa-tRNA
14.4 μM iVT aa-tRNA

Figure 3

A

HiBiT

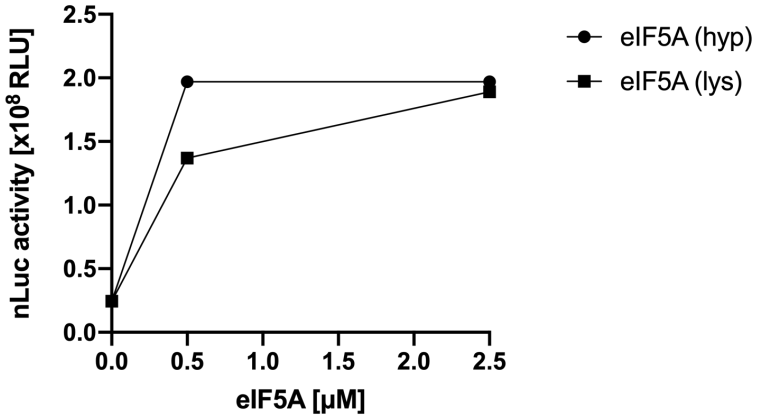

B

HiBiT

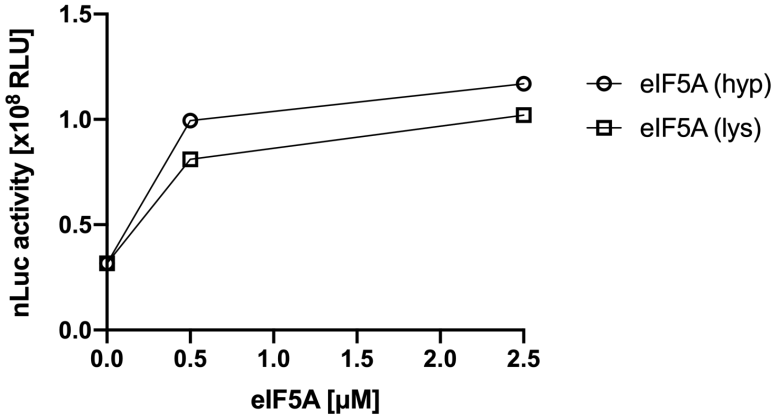

C

nLuc

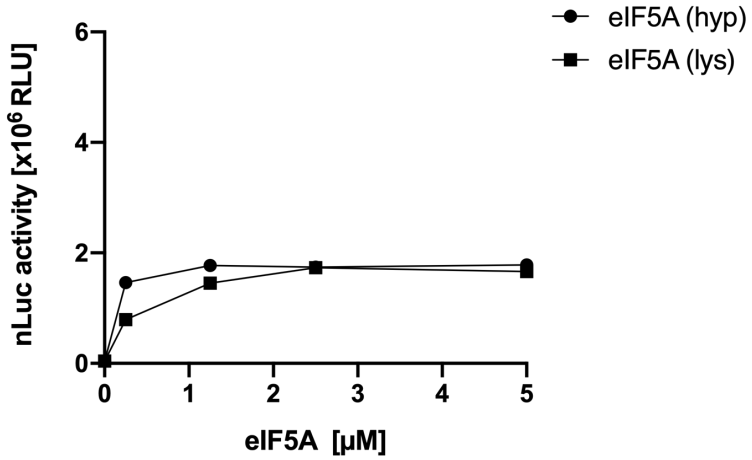

D

nLuc

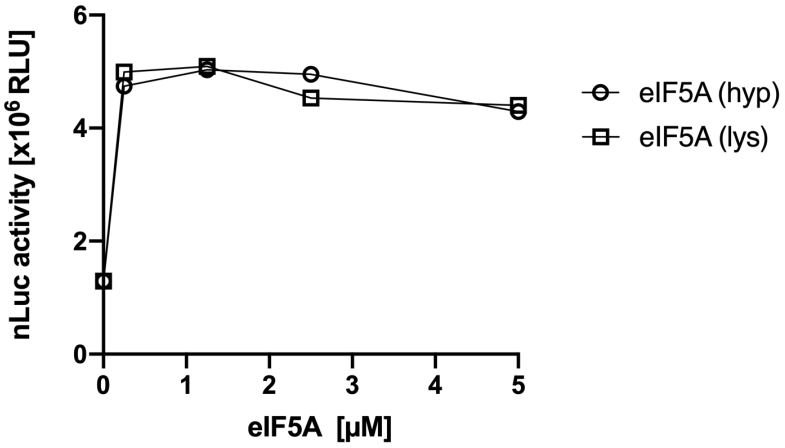

Figure 4

A

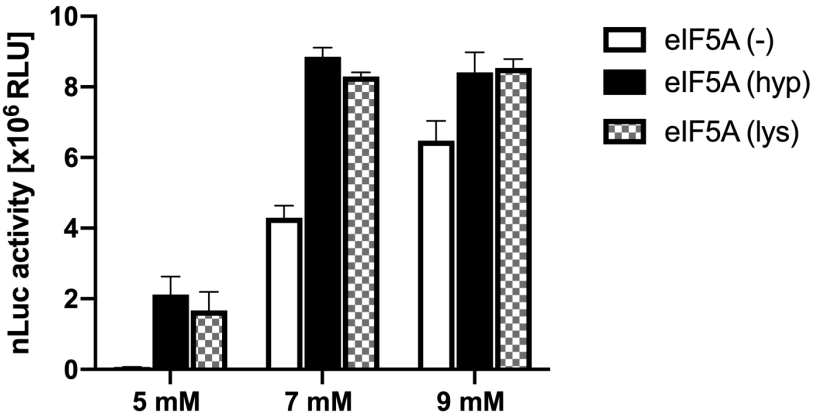

B

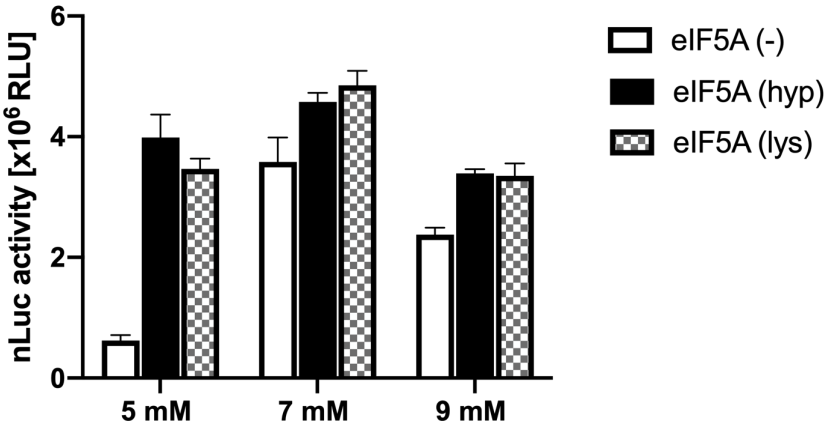

C

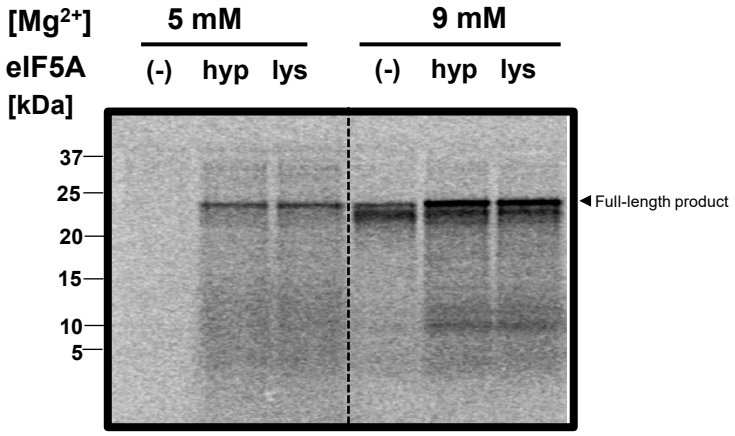

D

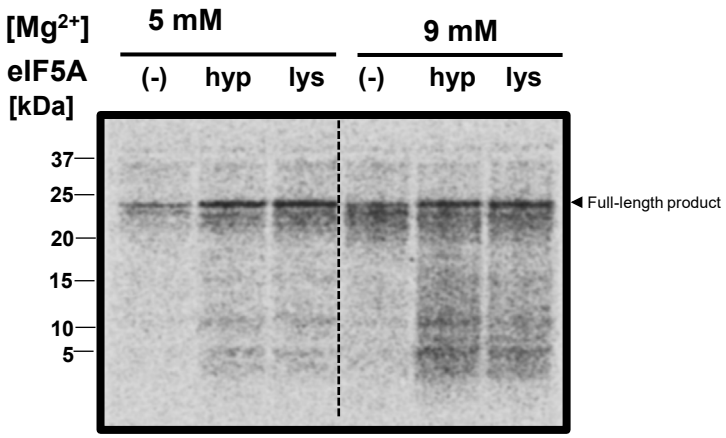

Figure 5

A

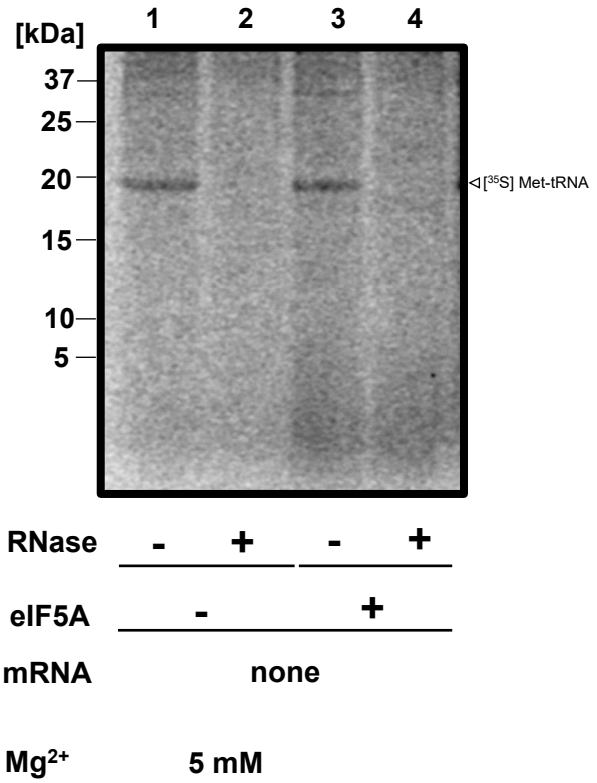

B

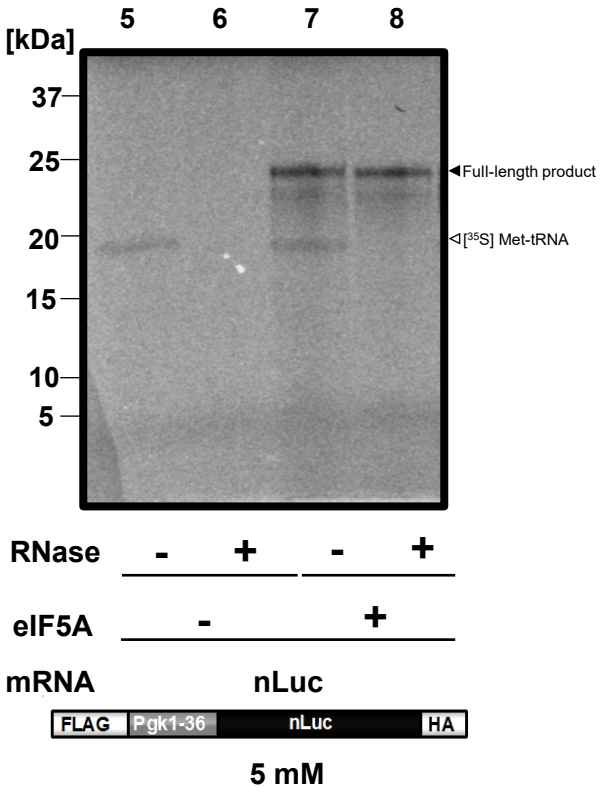

C

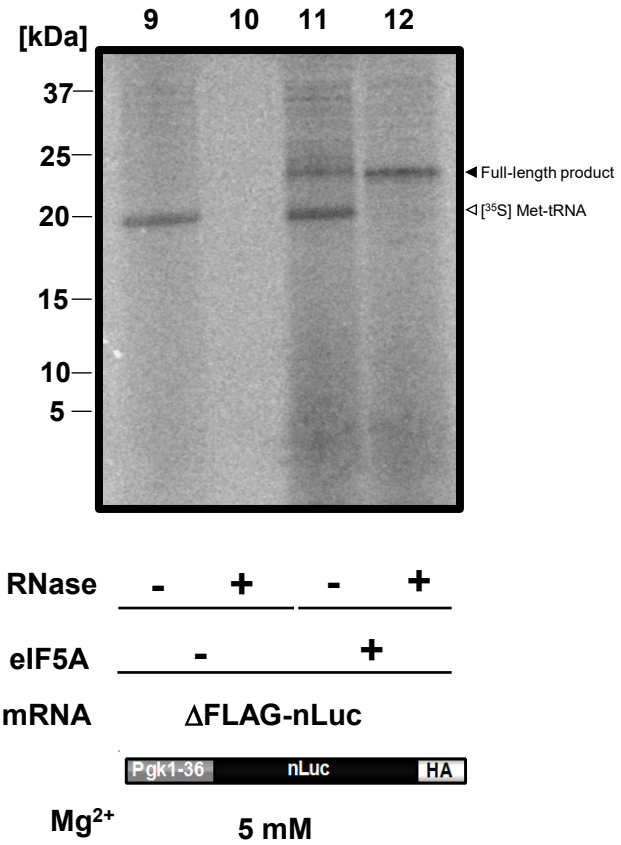

D

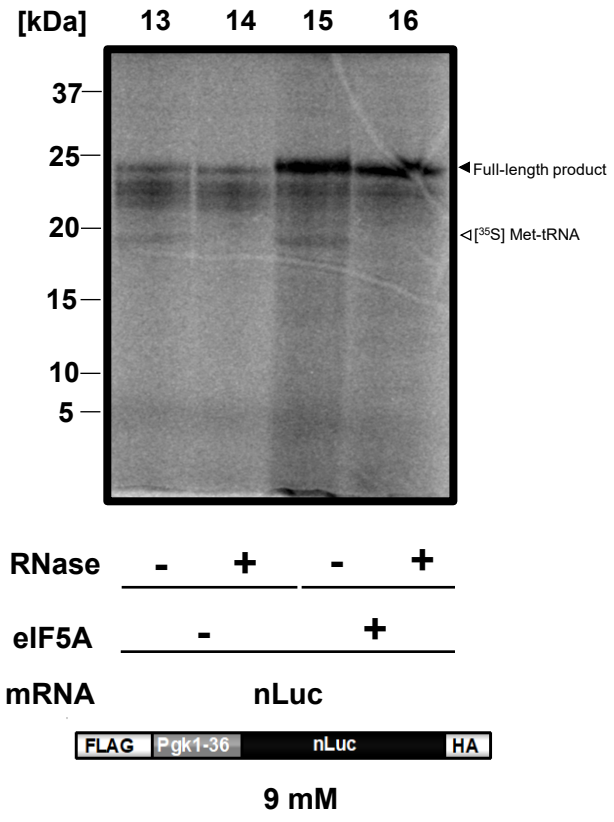

E

lane	2	4	6	8	10	12	14	16
nLuc activity [RLU]	1.20×10^{2}	1.00×10^{2}	3.6×10^{3}	2.46×10^{6}	8.53×10^{3}	7.32×10^{5}	5.54×10^{6}	8.36×10^{6}

Figure 6

A

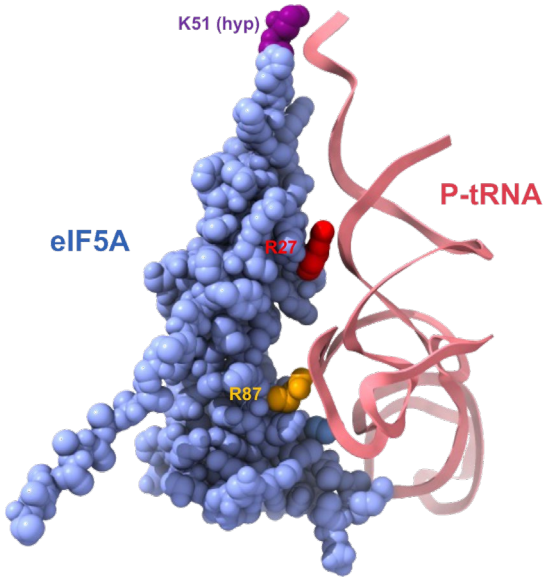
K51 (hyp)
P-tRNA
eIF5A
R27
R87

B

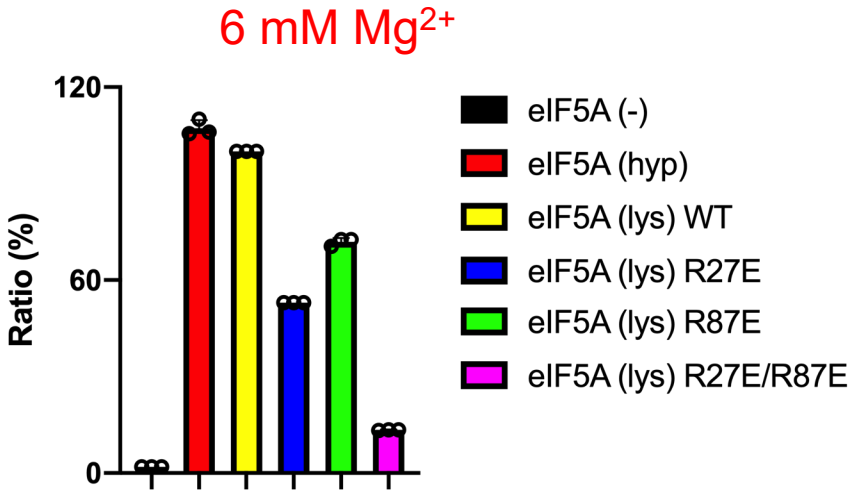
6 mM Mg2+
120
60
0
Ratio (%)
eIF5A (-)
eIF5A (hyp)
eIF5A (lys) WT
eIF5A (lys) R27E
eIF5A (lys) R87E
eIF5A (lys) R27E/R87E

C

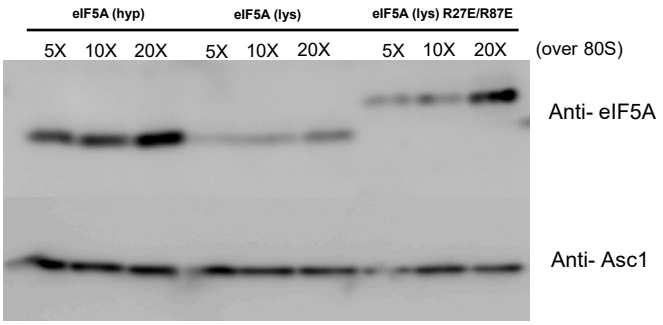
eIF5A (hyp)
eIF5A (lys)
eIF5A (lys) R27E/R87E
5X 10X 20X
5X 10X 20X
5X 10X 20X
(over 80S)
Anti- eIF5A
Anti- Asc1

Figure 7

no motif
Prox4
V

A

no motif

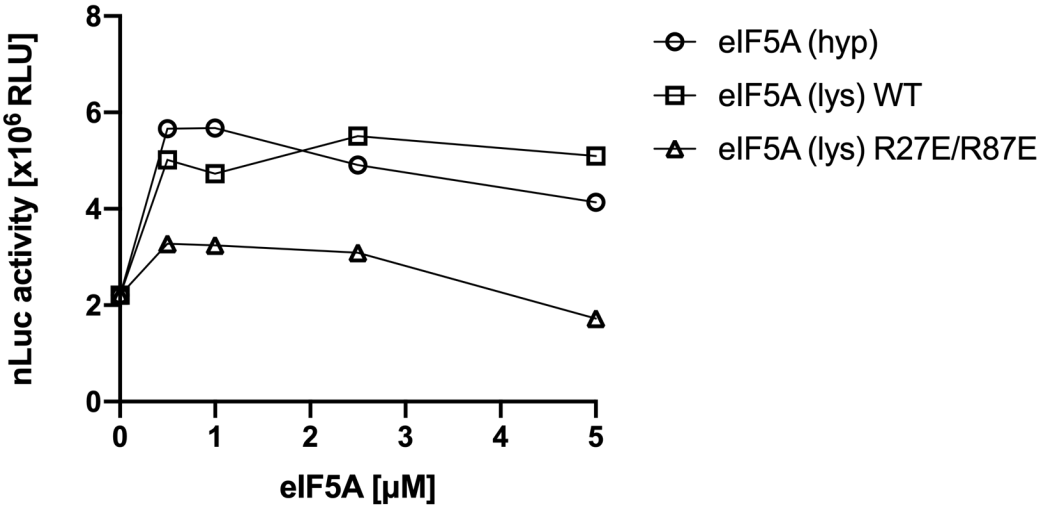

B

Pro x 4

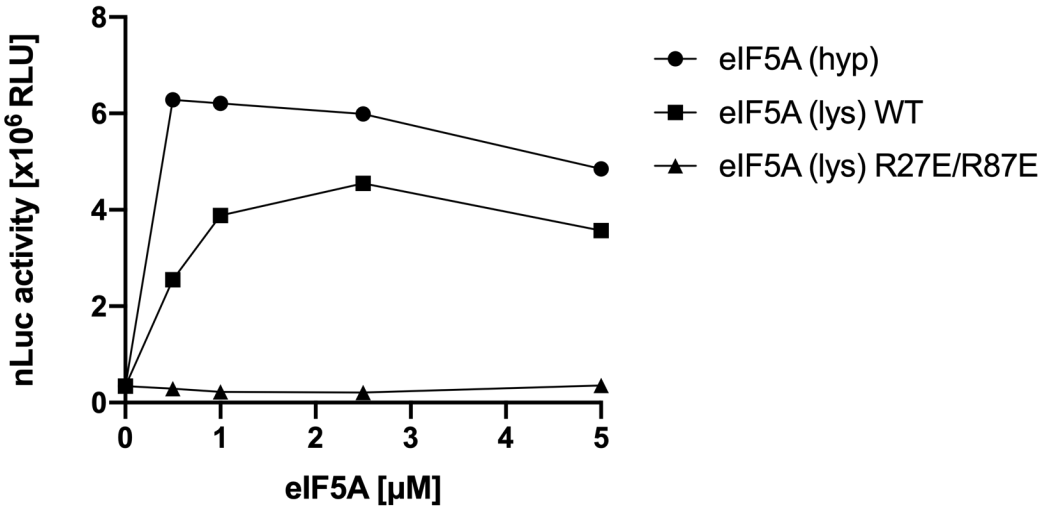

Figure 8
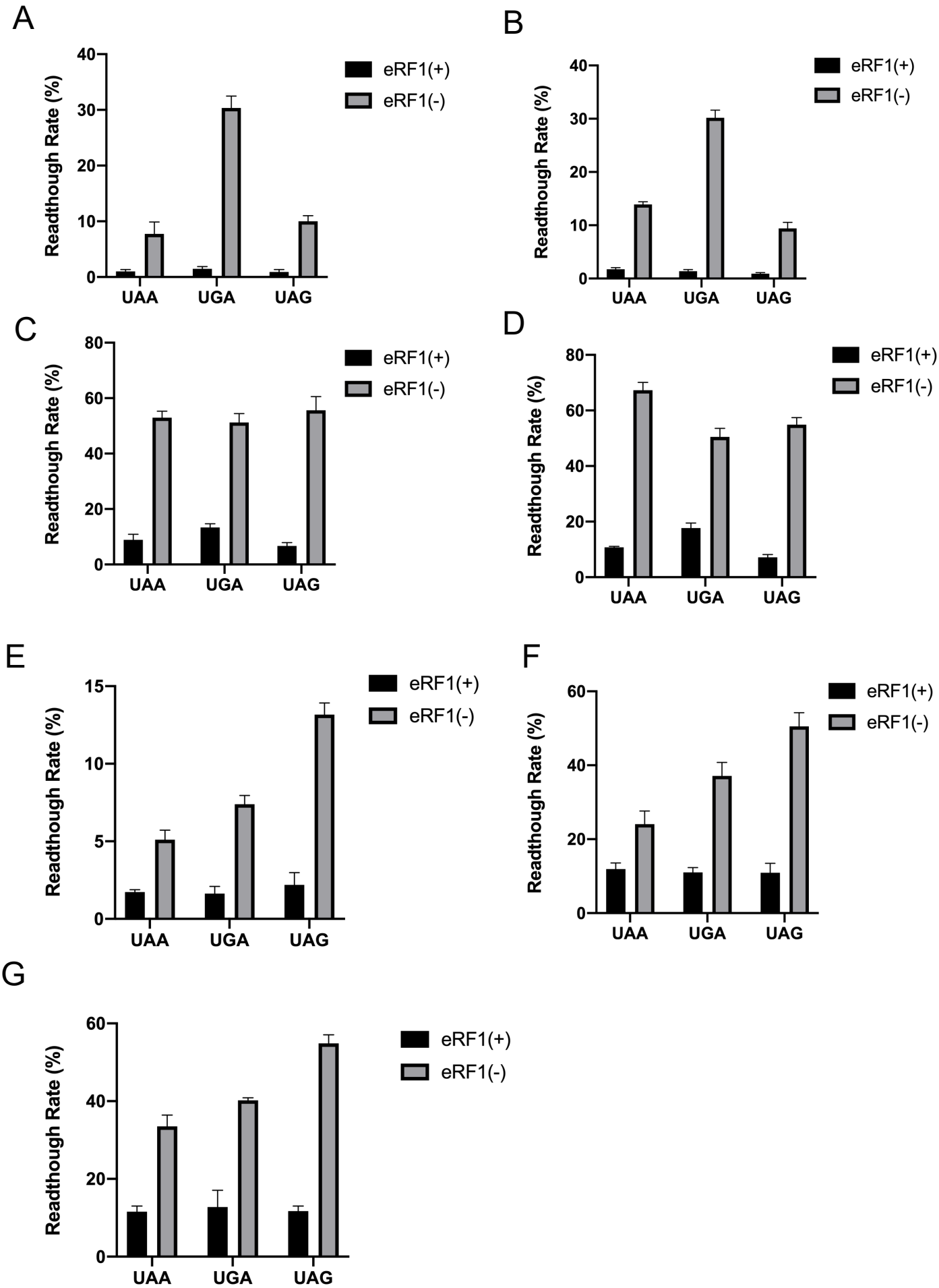
UAA / UGA / UAG
V